Ocean Engineering 137 (2017) 204–214

Contents lists available at ScienceDirect

Ocean Engineering

journal homepage: www.elsevier.com/locate/oceaneng

Design and simulation of X-rudder AUV's motion control

Yinghao Zhang, Yueming Li, Yushan Sun*, Jiangfeng Zeng, Lei Wan

Science and Technology on Underwater Vehicle Laboratory, Harbin Engineering University, Harbin, Heilongjiang 150001, China

ARTICLE INFO

Keywords:
AUV
X rudder
Virtual rudder
Rudder allocation
Ability judgment

ABSTRACT

This paper addresses the problem of motion control for autonomous underwater vehicles (AUVs) equipped with X rudder, in which all of the rudders can be operated independently. In order to offer accurate and reliable control ability, with the X rudder's character taken into consideration, one anti-normalization method based on virtual rudders and one rudder allocation including double-rudder, triple-rudder and quadruple-rudder modes are designed. Besides that, one new control ability judgment combined with traditional method and resistance energy is offered to find out the best control method. The simulations with different kinds of controllers under instantaneous and random disturbance are performed. In one simulation, one comparison with a cross-rudder AUV transformed from the test X-rudder AUV is also made. The results show that all of the designed X-rudder AUV motion control methods can complete the mission and the quadruple-rudder allocation has the best control ability.

1. Introduction

Underwater robotic vehicles (URVs) are widely used in the ocean engineering field. There are many classifications for URVs. Marine scientists and engineers usually classify them into remotely operated underwater vehicles (ROVs) (Chin, 2008) and autonomous underwater vehicles (AUVs) (Jon, 2013), according to whether there are control cables or not when these vehicles are under operation. Compared to ROVs, besides their differences in structure (Cheng, 2012), AUVs are not limited in the length of control cables (Wei-feng, 2008). With that help, AUVs are suitable for long-term and large-scale missions (Mahmoudian Nina, 2010), such as the mapping of underwater topography (Negre, 2014), collection of subsea hydrological data (Tadahiro, 2012), long oil pipe inspection (Lee, 2004), and even the naval mine detection (Hagen, 2006). The completion of all the missions is based on one foundation, namely the efficient and reliable motion control. For that purpose, numerous researchers try to offer their solutions and their solutions can mainly be classified into two kinds. The first kind is to develop or introduce new controllers in AUV's control. There are many controllers in theory or have already been used in some fields. Many AUV researchers try to use them to solve problems in AUV's motion control. Park (2015) presents a formation controller for desired formation of underactuated AUV with a new approach angel that requires only position information. Lei (2015) recommend active disturbance rejection control (ADRC) in AUV's bottom-following control to resistant the interference of external environment. /Lapierre and Jouvencel (2008) develop a robust nonlinear controller with backstepping and Lyapunov-based techniques for AUV's path-following control. The second kind is to design new control framework for AUVs. Usually, one AUV's control framework is composed by thrusters and rudders, especially the underacturated AUVs (Fang, 2010). However, some researchers try to design new control frameworks by the inspiration from marine creatures and other things, which can help AUVs finish some special missions. Ma (2015) design bionic pectoral fin, which can realize the combination of oscillating and chordwise twisting motion, as a new propelling way for AUVs. Tu (2015) design thrusters for one AUV whose control frame is only made up with thrusters, and this AUV's horizontal and vertical motions are just adjusted by the rotational speed of the thrusters. Jeong Sang-Ki (2016) design one underwater glider which is equipped with a controllable buoyancy engine to regulate the amount of buoyancy. With the thought of the second kind, besides the traditional cross rudder, some other kinds of rudders are adopted in underwater vehicles control, such as H style rudder and the rudder with flap (Shengda, 1995). X rudder is one of them.

The name of X rudder comes from the layout's shape. The rudders usually form the shape of X at the bow or stern of an AUV, so we call them the X rudder. According to literature's analysis, X rudder can be classified into the following three kinds:

- Fixed X rudder. The rudders of this kind X rudder can not be operated. An AUV named CR-02 designed by Tao (2002) is equipped with this kind of X rudder. The AUV's motion control is fulfilled by vertical and horizontal tunnel propellers and four main thrusters.

* Corresponding author.
E-mail address: sunyushan@hrbeu.edu.cn (Y. Sun).

http://dx.doi.org/10.1016/j.oceaneng.2017.03.048
Received 19 May 2016; Received in revised form 20 December 2016; Accepted 24 March 2017
Available online 05 April 2017

The X rudder's function is just to offer the extra stability when AUV is moving.

- Diagonal-linkage X rudder. This kind of X rudder is driven in the unit of a diagonal rudder pair, for example, the AUV named Yumeiruka designed by Yoshida (2013) Two X rudders are equipped at the bow and the stern of the AUV separately. The AUV can use them to cause the corresponding moments to control yaw and pitch. In March 2013, the 15-days sea trial of the AUV was carried out in the Sagami Bay.
- Independent X rudder. The rudders of this kind X rudder can be operated independently. This kind of X rudder is usually equipped on some countries' submarines, such as Gotland class (Gotland-class Submarine) from Sweden, Type 212 A (Type 212 Submarine) from Germany and Soryu class (Sōryū-class Submarine) from Japan. However, there are seldom public literature to describe their control methods. This kind of X rudder is also used in some torpedoes (Tiansen, 2007) and four rudders are usually operated at the same time in torpedoes control. Every rudder's operation in this X rudder can cause the changes of the vehicle's yaw and pitch together. In this paper, our study is focus on this kind of X rudder's use on AUV and we try to control part or all of X rudder at a time. To offer AUV more control styles means to give AUV more security.

The main contribution of this work is: From X rudder's control ability, we design the whole information framework of X-rudder AUV's motion control. Because the X rudder in this paper can be operated independently, its control ability is more flexible and multiple than traditional cross rudder. With X rudder's character taken into consideration, the anti-normalization method based on virtual rudders, rudder allocation method and a new control ability judgment standard to test the control results are designed. The rudder allocation also contains the double-rudder, triple-rudder and quadruple-rudder control modes. As AUV's energy is limited in one mission, when design quadruple-rudder mode, we also take energy saving into consideration.

The remainder of this paper is organized as follows: In Section 2, AUV's kinematics and dynamics equation is offered. In Section 3, the control method of X-rudder AUV is designed and analyzed. It mainly contains anti-normalization of X rudder, X rudder allocation and the control ability judgment. In Section 4, two simulations are designed to test the control ability of X rudder allocation. One is under instantaneous disturbance and the other one is under random disturbance. We also design one cross-rudder AUV which is transformed from the test X-rudder AUV and make one comparison simulation. In Section 5, we make a brief conclusion of this X rudder control method mentioned in this paper and our future plans.

2. Modelling of an X-rudder AUV

2.1. Coordinate systems

The test AUV's appearance and corresponding coordinate systems are shown in Fig. 1. To make it convenient in investigating the X rudder, two coordinates are designed according to Society of Naval Architects and Marine Engineers (SNAME). One is an inertial reference frame $E-\xi\eta\zeta(\{N\})$ and the other one is a body-fixed frame $O-xyz(\{B\})$. As to $\{N\}$, its original point E can be set at any place in the ocean. $E-\xi$ usually points to the AUV's main course, $E-\zeta$ points to the center of the earth and $E-\eta$ is vertical to the surface of $E-\xi\zeta$. As to $\{B\}$, its original point O is usually set at AUV's gravity center. $O-x$, $O-y$ and $O-z$ are the intersections of AUV's waterplane, buttock and transverse section. $O-x$ points to AUV's surge direction and $O-y$ points to AUV's starboard.

The test AUV's motion actuators are composed by one main thruster and one X rudder, whose four rudders can move individually. The rudders are laid out at the AUV's stern as the shape of X.

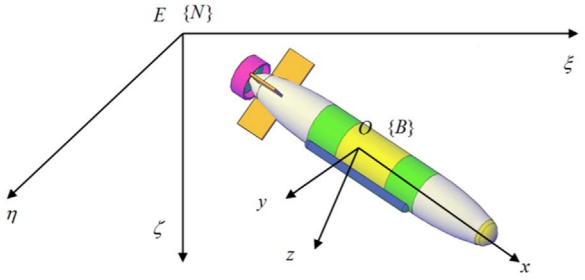

Fig. 1. X-rudder AUV and coordinate systems.

2.2. Kinematics and dynamics

According to reference (Chin, 2011; Fossen, 2011), we design the kinematics and dynamics equations. They are shown as Eqs. (1) and (2) separately.

$$\begin{cases}\dot{\xi}=u\cos\psi\cos\theta+v(\cos\psi\sin\theta\sin\phi-\sin\psi\cos\phi)\\ \quad+w(\cos\psi\sin\theta\sin\phi+\sin\psi\cos\phi)\\ \dot{\eta}=u\sin\psi\cos\theta+v(\sin\psi\sin\theta\sin\phi+\cos\psi\cos\phi)\\ \quad+w(\sin\psi\sin\theta\cos\phi-\cos\psi\cos\phi)\\ \dot{\zeta}=-u\sin\theta+v\cos\theta\sin\phi+w\cos\theta\cos\phi\\ \dot{\phi}=p+q\tan\theta\sin\phi+r\tan\theta\cos\phi\\ \dot{\theta}=q\cos\phi-r\sin\phi\\ \dot{\psi}=(q\sin\phi+r\cos\phi)/\cos\theta\end{cases}\tag{1}$$

$$\begin{cases}\dot{u}=X_{uu}u^2+X_{vv}v^2+X_{ww}w^2+X_{qq}q^2+X_{rr}r^2+X_{vr}vr+X_{wq}wq\\ \quad+X_{pr}pr+X+g_X/m+f_X/m\\ \dot{v}=Y_{\dot{p}}\dot{p}+Y_{\dot{r}}\dot{r}+Y_{v}uv+Y_{p}up+Y_{r}ur+Y_{vw}vw+Y_{v|v|}v|(v^2+w^2)^{1/2}|\\ \quad+Y_{v|\dot{r}|}(v/|v|)|(v^2+w^2)^{1/2}||r|+Y_{wp}wp+Y_{pq}pq+Y_{r|r|}r|r|+Y\\ \quad+g_Y/m+f_Y/m\\ \dot{w}=Z_{\dot{q}}\dot{q}+Z_{w}uw+Z_{|w|}u|w|+Z_{q}uq+Z_{vv}v^2+Z_{vp}vp+Z_{q|q|}q|q|+Z_{pp}p^2\\ \quad+Z_{pr}pr+Z_{ww}|w(v^2+w^2)^{1/2}|+Z_{w|w|}w|(v^2+w^2)^{1/2}|\\ \quad+Z_{w|q|}(w/|w|)|(v^2+w^2)^{1/2}||q|+Z+g_Z/m+f_Z/m\\ \dot{p}=K_{\dot{v}}\dot{v}+K_{\dot{r}}\dot{r}+K_{v}uv+K_{p}up+K_{r}ur+K_{vw}vw+K_{v|v|}v|(v^2+w^2)^{1/2}|\\ \quad+K_{vq}vq+K_{wp}wp+K_{wr}wr+K_{p|p|}p|p|+K_{pq}pq+K_{qr}qr+K_{r|r|}r|r|\\ \quad+K_{\phi}\cos\theta\sin\phi+K+g_K/I_x+f_K/I_x\\ \dot{q}=M_{\dot{w}}\dot{w}+M_{w}uw+M_{|w|}u|w|+M_{q}uq+M_{vv}v^2+M_{vp}vp+M_{pr}pr\\ \quad+M_{vr}vr+M_{ww}|w(v^2+w^2)^{1/2}|+M_{w|w|}w|(v^2+w^2)^{1/2}|+M_{pp}p^2\\ \quad+M_{wq}|(v^2+w^2)^{1/2}|q+M_{q|q|}q|q|+M_{rr}r^2+M+g_M/I_y+f_M/I_y\\ \dot{r}=N_{\dot{v}}\dot{v}+N_{\dot{p}}\dot{p}+N_{v}uv+N_{p}up+N_{r}ur+N_{vw}vw+N_{v|v|}v|(v^2+w^2)^{1/2}|\\ \quad+N_{v|r|}|(v^2+w^2)^{1/2}|r+N_{vq}vq+N_{wp}wp+N_{pq}pq+N_{qr}qr+N_{r|r|}r|r|\\ \quad+N+g_N/I_z+f_N/I_z\end{cases}\tag{2}$$

Where

ξ, η and ζ represent AUV's position in $E-\xi$, $E-\eta$ and $E-\zeta$. ϕ, θ and ψ represent AUV's roll angle, pitch angle and yaw angle in $\{N\}$. u, v and w represent AUV's speed in $O-x$, $O-y$ and $O-z$. p, q and r represent AUV's angular velocity in $O-x$, $O-y$ and $O-z$. X, Y and Z represent the force of AUV's motion executers in $E-\xi$, $E-\eta$ and $E-\zeta$. K M and N represent the moment of AUV's motion executers in $E-\xi$, $E-\eta$ and $E-\zeta$. g_* and f_* residual buoyancy's

Table 1
Some parameters in kinematics and dynamics equations.

Form	Effects on control performance	
R_*	The effect of fluid inertia force.	R represents X , Y, Z, K, M or N.
R_*	The effect of fluid viscosity force.	
R_{**}	If * and * are the same, it means the effect of fluid viscosity force. If * and * are different, it means the effect of coupling force.	* represents u, v, w, p, q or r.

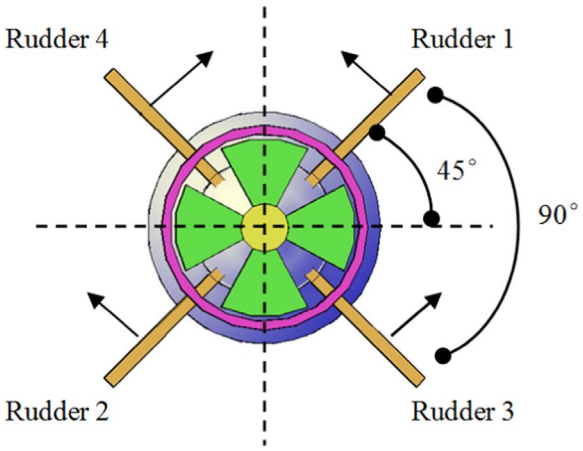

Fig. 2. Layout of X rudder.

and environment disturbance's effect to *. I_* represents AUV's moment of inertia to axis * in $\{B\}$. Other parameters' meanings are shown in Table 1.

We use $\boldsymbol{\tau} = [X, Y, Z, K, M, N]^T$ to represent the motion executors' inputs to AUV, and $\boldsymbol{\eta} = [\xi, \eta, \zeta, \phi, \theta, \psi]^T$ to represent AUV's position in $\{N\}$.

2.3. Layout of X rudder

Layout and serial numbers of the X rudder is shown in Fig. 2. Serial numbers will make it convenient to describe the control method. If the rudder can cause the corresponding force direction shown in Fig. 2, it means the rudder's angle is positive. Every rudder's appearance and rudder range are the same in X rudder.

In Fig. 2, we can find that the angle of adjacent rudders is 90°, which will significantly decline hydrodynamic disturbance of one rudder's operation to another. Besides that, the X rudder we mentioned here isn't comprised by fixed parts and movable parts as it is used in some submarines. When one rudder in X rudder is operated, it will move entirely. So that the rudder's hydrodynamic complexity in this X rudder is as similar as one traditional cross rudder's.

Eq. (3) shows the relationship between $\boldsymbol{\tau}$ and X-rudder AUV's motion executers.

$$\begin{cases} X = X_{\delta_1\delta_1} \times u^2 \times \delta_1{}^2 + X_{\delta_2\delta_2} \times u^2 \times \delta_2{}^2 + X_{\delta_3\delta_3} \times u^2 \times \delta_3{}^2 \\ \quad + X_{\delta_4\delta_4} \times u^2 \times \delta_4{}^2 + X_T \\ Y = Y_{\delta_1} \times u^2 \times \delta_1 + Y_{\delta_2} \times u^2 \times \delta_2 + Y_{\delta_3} \times u^2 \times \delta_3 + Y_{\delta_4} \times u^2 \times \delta_4 \\ Z = Z_{\delta_1} \times u^2 \times \delta_1 + Z_{\delta_2} \times u^2 \times \delta_2 + Y_{\delta_3} \times u^2 \times \delta_3 + Y_{\delta_4} \times u^2 \times \delta_4 \\ K = K_{\delta_1} \times u^2 \times \delta_1 + K_{\delta_2} \times u^2 \times \delta_2 + K_{\delta_3} \times u^2 \times \delta_3 + K_{\delta_4} \times u^2 \times \delta_4 \\ M = M_{\delta_1} \times u^2 \times \delta_1 + M_{\delta_2} \times u^2 \times \delta_2 + M_{\delta_3} \times u^2 \times \delta_3 + M_{\delta_4} \times u^2 \times \delta_4 \\ N = N_{\delta_1} \times u^2 \times \delta_1 + N_{\delta_2} \times u^2 \times \delta_2 + N_{\delta_3} \times u^2 \times \delta_3 + N_{\delta_4} \times u^2 \times \delta_4 \end{cases} \quad (3)$$

Where
X_T is the force of the main thruster.X_*, Y_*, Z_*, K_*, M_* and N_* are the corresponding parameters related to the rudders in X rudder. δ_* represents Rudder *'s angle. Eq. (3) shows X rudder's control performance in one AUV.

In Eq. (3) we can find that the main thruster can only influence the X in $\boldsymbol{\tau}$, and the X rudder can influence all of the elements in $\boldsymbol{\tau}$, which shows X rudder's flexibility and motility in AUV's control to some extent. X rudder's influence to X can be adjusted by X_T during the control of u in V. X rudder's influence on Y and Z can change v and w directly. However, v and w are not the main variables we are concerned with here. So in this paper, we will pay more attention to the design of a proper X rudder control method and the establishment of the mapping between $[\delta_1, \delta_2, \delta_3, \delta_4]$ and expected $[\phi, \theta, \psi]$ in $\boldsymbol{\eta}$.

As to X-rudder AUV, $m_{AUV} = 1420kg, l_{AUV} = 6m, I_x = 17kgm^2$, $I_y = 1835kgm^2, I_z = 1800kgm^2$ and some other main parameters about X rudder are shown in Table 2. Corresponding hydrodynamic parameters' values in Eqs. (2) and (3) are calculated by computational fluid dynamics methods in FLUENT.

3. Control of an AUV with X rudder

3.1. Differences between cross rudder and X rudder in control flow

Usually, if an AUV is controlled by cross rudder and control law is based on error (e) and the rate of error ($\dot{e}$) , the heading and depth control information can be described as Fig. 3.

Normalization and Anti-normalization should be used together. Normalization can limit the output of control law between −1 and 1. With the help of that, we can just use small adjustment of control parameters to get big changes of output. That will help us to get corresponding parameters' ranges in short time. As the real output of control law is not just between −1 and 1, we need to use the Anti-normalization part to get the answers. The module of Depth to pitch is used to change the depth control to pitch control. It can be designed as Eq. (4).

$$\theta_{expect} = \arctan((\zeta - \zeta_{expect})/(l_{AUV} \times n)),\ n > 0 \quad (4)$$

Where
ζ_{expect} is the expected depth, l_{AUV} is the length of AUV, n is a changeable parameter and θ_{expect} is the expected pitch angle.

As to the X rudder control, there are two unique problems: one is the problem of anti-normalization and the other one is the problem of rudder allocation. They will be introduced in the following parts.

Table 2
Main parameters of the X rudder.

$X_{\delta_1\delta_1}$	-5.0303×10^{-4}	Y_{δ_1}	-3.8375×10^{-4}	Z_{δ_1}	-6.6442×10^{-4}	K_{δ_1}	-1.5876×10^{-3}	M_{δ_1}	-5.6597×10^{-5}	N_{δ_1}	5.2033×10^{-5}
$X_{\delta_2\delta_2}$	-5.0303×10^{-4}	Y_{δ_2}	-3.8375×10^{-4}	Z_{δ_2}	-6.6442×10^{-4}	K_{δ_2}	1.5876×10^{-3}	M_{δ_2}	-5.6597×10^{-5}	N_{δ_2}	5.2033×10^{-5}
$X_{\delta_3\delta_3}$	-5.6451×10^{-4}	Y_{δ_3}	4.6028×10^{-4}	Z_{δ_3}	-7.3760×10^{-4}	K_{δ_3}	-2.0030×10^{-3}	M_{δ_3}	-6.8421×10^{-5}	N_{δ_3}	-6.7854×10^{-5}
$X_{\delta_4\delta_4}$	-5.6451×10^{-4}	Y_{δ_4}	4.6028×10^{-4}	Z_{δ_4}	-7.3760×10^{-4}	K_{δ_4}	2.0030×10^{-3}	M_{δ_4}	-6.8421×10^{-5}	N_{δ_4}	-6.7854×10^{-5}

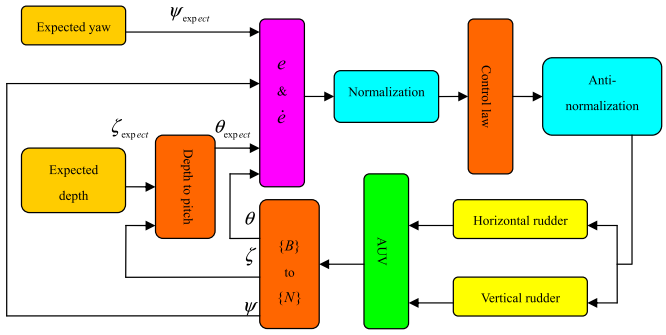

Fig. 3. The information framework of cross-rudder AUV's motion control.

3.2. Anti-normalization of X rudder

As to the cross-rudder AUV, the process of anti-normalization is very clear and comprehensible. For example, if we want to control heading and pitch, we can use Eq. (5).

$$\begin{cases} \delta_v = CTR_{yaw,cross} \times \delta_{v,\max} \\ \delta_h = CTR_{pitch,cross} \times \delta_{h,\max} \\ -1 \le CTR_{yaw,cross},\ CTR_{pitch,cross} \le +1 \end{cases} \tag{5}$$

Where
$CTR_{yaw,cross}$ and $CTR_{pitch,cross}$ are the outputs of corresponding control laws. $\delta_{v,\max}$ and $\delta_{h,\max}$ are the maximal values of the vertical rudder and horizontal rudder. δ_v and δ_h are the cross rudder we need.

As to the X-rudder AUV, the process of anti-normalization is a little confusing. We can not arrange the certain angle to the certain rudder in X rudder directly. Because any operation of the rudder in X rudder can cause changes in $\boldsymbol{\tau}$, which is very complex, especially to $[K, M, N]$. So, considering practicability and operability, we design the anti-normalization method based on virtual rudders shown in Eq. (6).

$$\boldsymbol{\delta}_{VR} = \boldsymbol{M}_{CTR}\delta_{AN}\boldsymbol{M}_I \tag{6}$$

Where
$\boldsymbol{\delta}_{VR} = [\delta_{VR,roll}, \delta_{VR,pitch}, \delta_{VR,yaw}]^T$. $\delta_{VR,roll}$,$\delta_{VR,pitch}$ and $\delta_{VR,yaw}$ are the virtual rudders of controlling roll, pitch and yaw separately. $\boldsymbol{M}_{CTR} = diag(CTR_{roll}, CTR_{pitch}, CTR_{yaw})$,
$-1 \le CTR_{roll}, CTR_{pitch}, CTR_{yaw} \le +1$.
CTR_{roll}, CTR_{pitch} and CTR_{yaw} represent the outputs of corresponding control laws of roll, pitch and yaw. δ_{AN} is one anti-normalization angle, according to test results, it can be set between 75% and 150% the range of rudders in X rudder. $\boldsymbol{M}_I = [I_{roll}, I_{pitch}, I_{yaw}]$. I_{roll}, I_{pitch} and I_{yaw} are adjustable parameters. They represent the control priority in roll, pitch and yaw, i.e., the greater element in $\boldsymbol{M}_I$, means the greater priority of the corresponding motion control.

Anti-normalization's purpose is to find out the right $\boldsymbol{\delta}_{VR}$. Even though it is not real and X rudder is the real reason which can affect $[K, M, N]$, $\boldsymbol{\delta}_{VR}$ is the foundation of rudder allocation and rudder allocation is the bridge between $\boldsymbol{\delta}_{VR}$ and X rudder.

3.3. Rudder allocation of X rudder

The angles of every rudders, which are responsible for X-rudder AUV's motion, can be calculated by the rudder allocation. Because every rudder in X rudder can be operated independently, there are a lot of combinations. If the combinations are classified according to the number of rudders taken part in AUV's motion control, there can be three types, i.e. double-rudder allocation, triple-rudder allocation and quadruple-rudder allocation. The total combination number of them is $C_4^2 + C_4^3 + C_4^4 = 11$. We can't analyze all of them due to the limited length of this paper. However, we can design and analyze double-rudder, triple-rudder and quadruple-rudder modes with certain examples.

3.3.1. Double-rudder allocation (DR)

When there are two rudders responsible for X-rudder AUV's motion control, this belongs to the under-actuated control. There are three variables ($[\phi, \theta, \psi]$) needed to be controlled, however, only two rudders can be used. When dealing with the under-actuated situation, we usually have priorities, i.e. to control the significant variables first. As to AUV's motion control, we consider heading control and depth control most. According to Section 3.1, depth control can be turned to pitch control. So that if we want to use DR method, we should pay attention to the control of ψ and θ. We will use Rudder 1 and Rudder 3 for example. Considering the research in Sections 2.3 and 3.2, we can design the following DR method.

$$\begin{cases} M_{\delta_1} \times \delta_1 + M_{\delta_3} \times \delta_3 = \delta_{VR,pitch} \\ N_{\delta_1} \times \delta_1 + N_{\delta_3} \times \delta_3 = \delta_{VR,yaw} \\ \underline{\delta} \le \delta_1,\ \delta_3 \le \overline{\delta} \end{cases} \tag{7}$$

Where
$\underline{\delta}$ and $\overline{\delta}$ represent the minimal rudder and maximal. δ_1 and δ_3 are the X rudders we need. If the calculation result of δ_1 or δ_3 is beyond rudder's range, we can use the truncation method, which is to make the rudder angle equal to the maximum or minimum value. M_* and N_* are shown in Eq. (3). $\delta_{VR,pitch}$ and $\delta_{VR,yaw}$ are shown in Eq. (6).

3.3.2. Triple-rudder allocation (TR)

When there are three rudders responsible for X-rudder AUV's motion control, this belongs to the full-actuated control. There are three variables ($[\phi, \theta, \psi]$) needed to be controlled and there are also three rudders can be used. We will use Rudder 1, Rudder 2 and Rudder 3 for example. Considering the control of yaw, depth and roll, we can design the following TR method.

$$\begin{cases} K_{\delta_1} \times \delta_1 + K_{\delta_2} \times \delta_2 + K_{\delta_3} \times \delta_3 = \delta_{VR,roll} \\ M_{\delta_1} \times \delta_1 + M_{\delta_2} \times \delta_2 + M_{\delta_3} \times \delta_3 = \delta_{VR,pitch} \\ N_{\delta_1} \times \delta_1 + N_{\delta_2} \times \delta_2 + N_{\delta_3} \times \delta_3 = \delta_{VR,yaw} \\ \underline{\delta} \le \delta_1,\ \delta_2,\ \delta_3 \le \overline{\delta} \end{cases} \tag{8}$$

Where
K_*, M_* and N_* are shown in Eq. (3). $\delta_{VR,roll}$,$\delta_{VR,pitch}$ and $\delta_{VR,yaw}$ are shown in Eq. (6).

If the calculation result of δ_1, δ_2 or δ_3 is beyond corresponding range of rudder, we can use the truncation method, which is the same as DR.

3.3.3. Quadruple-rudder allocation (QR)

When there are four rudders responsible for X-rudder AUV's motion control, this belongs to the over-actuated control. There are three variables ($[\phi, \theta, \psi]$) which need to be controlled and more than three rudders can be used. In this situation, we try to design QR method to solve the problem shown as follows.

$$\begin{cases} K_{\delta_1} \times \delta_1 + K_{\delta_2} \times \delta_2 + K_{\delta_3} \times \delta_3 + K_{\delta_4} \times \delta_4 = \delta_{VR,roll} \\ M_{\delta_1} \times \delta_1 + M_{\delta_2} \times \delta_2 + M_{\delta_3} \times \delta_3 + M_{\delta_4} \times \delta_4 = \delta_{VR,pitch} \\ N_{\delta_1} \times \delta_1 + N_{\delta_2} \times \delta_2 + N_{\delta_3} \times \delta_3 + N_{\delta_4} \times \delta_4 = \delta_{VR,yaw} \\ \underline{\delta} \le \delta_1,\ \delta_2,\ \delta_3,\ \delta_4 \le \overline{\delta} \end{cases} \tag{9}$$

In order to simplify Eq. (9), we change it into the following form and make corresponding assumptions.

$$\begin{cases} \boldsymbol{B}\boldsymbol{u}_\delta = \boldsymbol{\delta}_{VR} \\ \text{Assuming:} \\ -1 \le \delta_1,\ \delta_1,\ \delta_1,\ \delta_1 \le +1 \\ -1 \le \delta_{VR,roll},\ \delta_{VR,pitch},\ \delta_{VR,yaw} \le +1 \end{cases} \tag{10}$$

Where
$\boldsymbol{B} = [K_{\delta_1}K_{\delta_2}K_{\delta_3}K_{\delta_4}, M_{\delta_1}M_{\delta_2}M_{\delta_3}M_{\delta_4}, N_{\delta_1}N_{\delta_2}N_{\delta_3}N_{\delta_4}]^T$,$\boldsymbol{u}_\delta = [\delta_1, \delta_2, \delta_3, \delta_4]^T$. K_*, M_* and N_* are shown in Eq. (3). $\boldsymbol{\delta}_{VR}$ is mentioned in Eq. (6). The

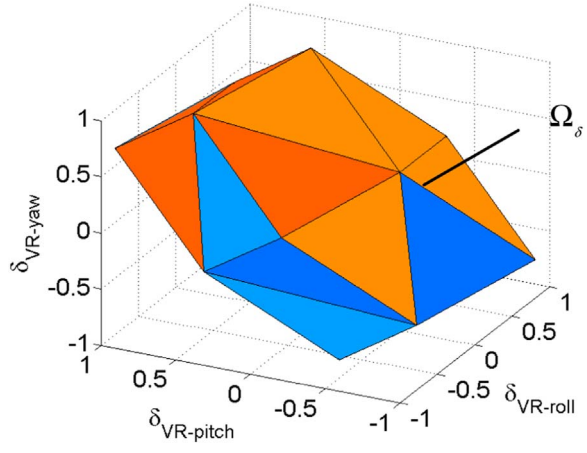

Fig. 4. The space of $\boldsymbol{u}_\delta$'s reasonable solution set.

assumptions will simplify the description of QR design and the units of variables will not be mentioned in this section because the results will not be affected by them.

In order to solve the problem as Eq. (10), we usually use the method of pseudoinverse (Fossen, 2002) shown in Eq. (11).

$$\boldsymbol{u}_\delta = \boldsymbol{B}^+\boldsymbol{\delta}_{VR},\ \boldsymbol{B}^+ = \boldsymbol{B}^T(\boldsymbol{B}\boldsymbol{B}^T)^{-1} \tag{11}$$

Where

$\boldsymbol{B}^+$ is the pseudoinverse of $\boldsymbol{B}$. As $\boldsymbol{u}_\delta$ is four dimensional, and it's difficult to show directly, so we try to build the direct relationship in three dimensional space according to Eq. (10). The relationship between reasonable solution set of $\boldsymbol{u}_\delta$ and $\boldsymbol{\delta}_{VR}$ can be shown in Fig. 4. In Fig. 4, the reasonable solution set of $\boldsymbol{u}_\delta$ in space $\boldsymbol{\delta}_{VR}$ is represented by Ω_δ.

According to Eq. (11), we can get one answer of $\boldsymbol{u}_\delta$. However, the solution of pseudoinverse doesn't consider the reasonable solution set of $\boldsymbol{u}_\delta$. That can make the result of pseudoinverse one of the following two situations,

I. The solution of pseudoinverse is on the boundary of space Ω_δ or in space Ω_δ. It means the solution fits the requirement, but we are not sure if it's the only answer or the best answer.
II. The solution of pseudoinverse is out of space Ω_δ. It means the solution doesn't fit the requirement.

If the result of pseudoinverse belongs to situation I, in order to find out the precise answer, we introduce the criterion of the least energy (Burken, 2001) shown in Eq. (12).

$$\min J = (1-\varepsilon)\|\boldsymbol{W}_v(\boldsymbol{B}\boldsymbol{u}_\delta - \boldsymbol{\delta}_{VR})\|_2^2 + \varepsilon\|\boldsymbol{W}_u(\boldsymbol{u}_\delta - \boldsymbol{u}_{\delta d})\|_2^2,$$
$$\underline{\delta} \le \boldsymbol{u}_\delta \le \overline{\delta},\ 0<|\varepsilon|<1 \tag{12}$$

Where

ε is an adjustable parameter. $\boldsymbol{u}_{\delta d}$ is $\boldsymbol{u}_\delta$'s expected value.$\boldsymbol{W}_v$ and $\boldsymbol{W}_u$ are diagonal weight matrixes, and their dimension is decided by the dimension of $\boldsymbol{u}_\delta$. In X rudder's control, $\boldsymbol{W}_v$ and $\boldsymbol{W}_u$ can be set as:

$$W_v = diag(1/\delta_{VR,roll\ \max},\ 1/\delta_{VR,pitch\ \max},\ 1/\delta_{VR,yaw\ \max}),\ W_u$$
$$= diag(1/\delta_{1\ \max},\ 1/\delta_{2\ \max},\ 1/\delta_{3\ \max},\ 1/\delta_{4\ \max}).$$

Before solving the problem of Eq. (12), we can simplify J first. If $\boldsymbol{u}_{\delta d}$ in J is equal to $\boldsymbol{0}$, it means we want the rudders to make the minimum movements and Eq. (12) can be transformed as Eq. (13).

$$\min J = (1-\varepsilon)\|\boldsymbol{W}_v(\boldsymbol{B}\boldsymbol{u}_\delta - \boldsymbol{\delta}_{VR})\|_2^2 + \varepsilon\|\boldsymbol{W}_u\boldsymbol{u}_\delta\|_2^2$$
$$= (1-\varepsilon)(\boldsymbol{B}\boldsymbol{u}_\delta - \boldsymbol{\delta}_{VR})^T\boldsymbol{Q}_1(\boldsymbol{B}\boldsymbol{u}_\delta - \boldsymbol{\delta}_{VR}) + \varepsilon\boldsymbol{u}_\delta{}^T\boldsymbol{Q}_2\boldsymbol{u}_\delta \tag{13}$$

Where

$\boldsymbol{Q}_1 = \boldsymbol{W}_v{}^T\boldsymbol{W}_v$, $\boldsymbol{Q}_2 = \boldsymbol{W}_u{}^T\boldsymbol{W}_u$. If we find the $\boldsymbol{u}_\delta$ which fits Eq. (13), then we will find the answer. In order to solve the problem of Eq. (13) with the solution of pseudoinverse mentioned before, we decide to use the method of fixed point iteration. According to the contraction mapping theorem (Chun, 2012), we try to design Eq. (14) to solve the problem of minimum J.

$$\boldsymbol{u}_{\delta n+1} = sat[(1-\varepsilon)\omega\boldsymbol{B}^T\boldsymbol{Q}_1\boldsymbol{\delta}_{VR} - (\omega\boldsymbol{H} - \boldsymbol{I})\boldsymbol{u}_{\delta n}] \tag{14}$$

Where

$\boldsymbol{H} = (1-\varepsilon)\boldsymbol{B}^T\boldsymbol{Q}_1\boldsymbol{B} + \varepsilon\boldsymbol{Q}_2$. $\omega = 1/\|\boldsymbol{H}\|_2$. $\boldsymbol{I} = diag(1, 1, 1, 1)$. $\boldsymbol{u}_{\delta n}$ and $\boldsymbol{u}_{\delta n+1}$ mean $\boldsymbol{u}_\delta$ in the nth iteration and the $(n+1)th$ iteration. The definition of sat can be explained by Eq. (15).

$$sat(x) = \begin{cases} \underline{\delta}, & x \le \underline{\delta} \\ x, & \underline{\delta} < x < \overline{\delta} \\ \overline{\delta}, & x \ge \overline{\delta} \end{cases} \tag{15}$$

The solution of pseudoinverse, which is belong to situation I, can be the original iteration point $\boldsymbol{u}_{\delta 0}$ in this fixed point iteration. Besides that, the criterion of the iteration's end can be shown as Eq. (16).

$$|J(\boldsymbol{u}_{\delta k+1}) - J(\boldsymbol{u}_{\delta k})| \le J_{end} \tag{16}$$

Where

J_{end} is an adjustable parameter. Eq. (16) shows the situation of the kth iteration and $\boldsymbol{u}_{\delta k+1}$ is the answer we need.

If the result of pseudoinverse belongs to situation II, we could use the truncation method, forcing the corresponding part in the reasonable solution set of $\boldsymbol{u}_\delta$. Therefore, we can transform situation II to situation I. After that, we use the fixed point iteration mentioned before to calculate the proper answer of $\boldsymbol{u}_\delta$. The whole process of QR can be described by Fig. 5.

At this point, we've designed and analyzed all of the X rudder's combination categories. Thus, we can sum up information framework of X rudder control as Fig. 6.

3.4. The control ability judgment of X rudder

The traditional judgment about control ability is mainly concentrated in response time, number of oscillations and steady-state error. However, AUV must overcome the resistance energy caused by rudders to move, which means that the resistance energy shouldn't be ignored when we judge the rudder allocation, especially to the motion actuator as X rudder. So, we combine the traditional judgment standard and the resistance energy together, to design a new judgment of X rudder's allocation.

We define the following four variables, which are used in the control ability judgment. They are shown in Eq. (17).

$$\begin{cases} E_\alpha = \int_0^T |e_\alpha| dt \\ \mathrm{Re} = \int_0^T F_{re} udt = \int_0^T (\rho/2) \times C_D(v_f) \times {v_f}^2 \times S_{rudder} \times |\sin\delta| \times udt \\ \mathrm{Re}_{Total} = \sum \mathrm{Re}_* \\ \boldsymbol{M}_w = [M_{w1}, M_{w2}, \ldots, M_{wi}, \ldots, M_{wn}],\ \sum_{i=1}^n M_{wi} = 1 \text{and} 0 \le M_{wi} \le 1 \end{cases} \tag{17}$$

Where

In E_α, e is the control variable error between control result and

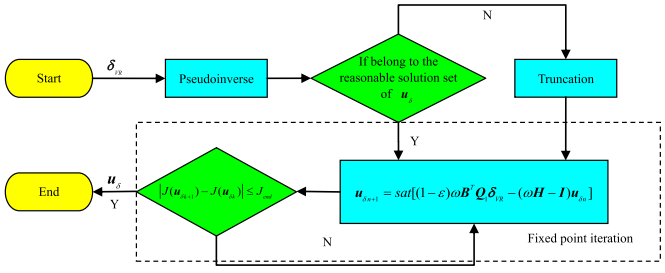

Fig. 5. The information framework of QR.

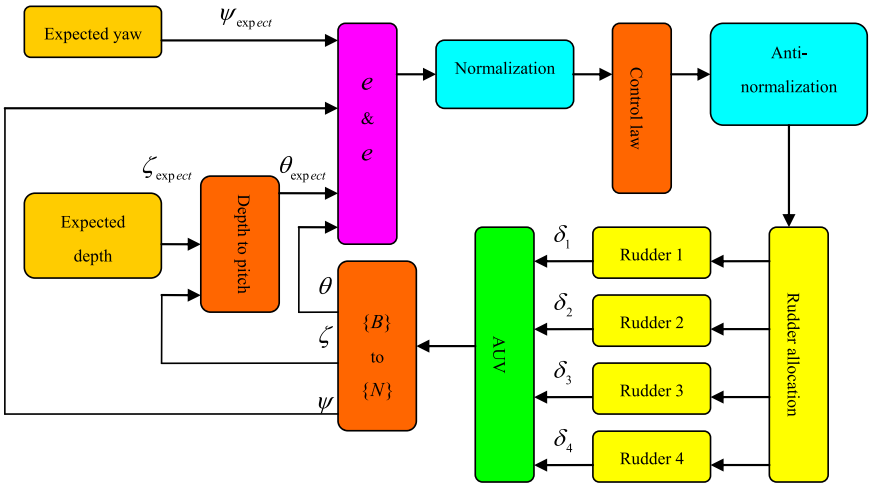

Fig. 6. The information framework of X-rudder AUV's motion control.

expected value. α represents the control variable, such as depth, yaw angle, roll angle, pitch angle and etc., which are needed to be compared. In Re, F_{re} is the resistance caused by one rudder's operation. ρ,C_D,u,v_f,S_{rudder} and δ represent density of environment, drag coefficient (Volker, 2000), AUV's velocity, flow velocity to rudder , area of the rudder and rudder angle separately. T is runtime. In Re_{Total}, * is the rudder's number, which is responsible for AUV's motion control. In $\boldsymbol{M}_w$, n is corresponding to the kinds of α. In the field trail , v_f can be tested by the flow meter equipped on AUV.

In Eq. (17), E_α is used to measure response time, number of oscillations and steady-state error at a time. If the trend of control results is nearly the same when rudder allocations are different, the smaller E_α means smaller measure response time, number of oscillations and steady-state error in the α control variable. Re is one rudder's resistance energy. If we want to evaluate the ability of one rudder allocation in the energy field, we also need to consider the number of the rudders that are responsible for AUV's motion control. Re_{Total} is the total resistance energy caused by the rudders in one rudder allocation. The smaller Re_{Total} means that the corresponding rudder allocation costs less energy during AUV's motion control and AUV can run for longer time. $\boldsymbol{M}_w$ is the weight matrix.

In this paper, the X rudder is designed based on NACA0012. Fig. 7 shows the whole C_D curve of NACA0012. Fig. 8 shows a part of C_D curve from 0° to 35° and the corresponding fitting curve can be described by Eq. (18).

$$C_D = \begin{cases} 0 & , \quad |\delta| < 5 \times pi/180 \\ 1.4083 \times |\delta|^2 + 0.4832 \times |\delta| - 0.0457, & 5 \times pi/180 \le |\delta| \\ & \le 35 \times pi/180 \end{cases} \tag{18}$$

Where
δ is rudder's angle in the unit of rad.

The following example will show how this judgment of rudder allocation combines E_α and Re_{Total}. If we want to compare the capability

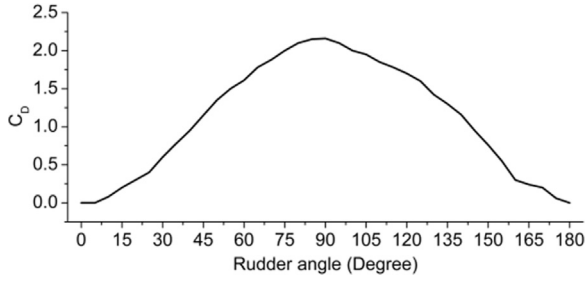

Fig. 7. C_D of NACA0012.

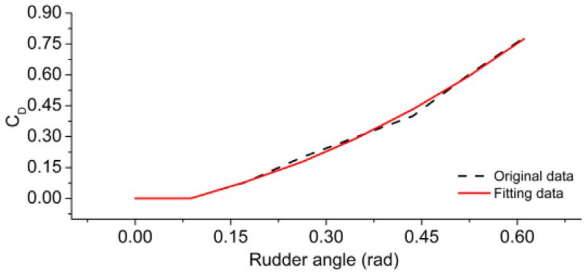

Fig. 8. A part of C_D and fitting curve.

Table 3
Preparation for ability judgment of X rudder.

Double-rudder (DR)	$E_{Depth.DR}$	$\mathrm{Re}_{Total.DR} = \mathrm{Re}_{1.DR} + \mathrm{Re}_{2.DR}$
Quadruple-rudder (QR)	$E_{Depth.QR}$	$\mathrm{Re}_{Total.QR} = \mathrm{Re}_{1.QR} + \mathrm{Re}_{2.QR} + \mathrm{Re}_{3.QR} + \mathrm{Re}_{4.QR}$

of double-rudder allocation (The rudders' numbers are 1 and 2.) and quadruple-rudder allocation (The rudders' numbers are 1,2,3 and 4) in depth control, we can set $\boldsymbol{M}_w = [M_{w1}, M_{w2}]$, and calculate the values shown in Table 3. M_{w1} and M_{w2} show the weights of traditional judgment standard and resistance energy in the final judgment results.

As to double-rudder allocation, the final judgment result is

$$A_{DR} = \boldsymbol{M}_w \bullet [E_{Depth.DR}/\max(E_{Depth.DR}, E_{Depth.QR}), \mathrm{Re}_{Total.DR}/\max(\mathrm{Re}_{Total.DR}, \mathrm{Re}_{Total.QR})]^T$$

$$0 \le A_{DR} \le 1.$$

As to Quadruple-rudder allocation, the final judgment result is

$$A_{QR} = \boldsymbol{M}_w \bullet [E_{Depth.QR}/\max(E_{Depth.DR}, E_{Depth.QR}), \mathrm{Re}_{Total.QR}/\max(\mathrm{Re}_{Total.DR}, \mathrm{Re}_{Total.QR})]^T$$

$$0 \le A_{QR} \le 1.$$

A_{DR} and A_{QR} are the digitization of traditional judgment standard and resistance energy. According to the analysis before, the less value of A_{DR} and A_{QR} are, the greater control ability the corresponding rudder allocation has.

4. Simulation results and analysis

4.1. Preparation for simulation

In Section 4, there are two simulations. In one simulation, we will simulate the whole process of following one lawn mower path in 3 dimension environment by different X rudder allocation methods and

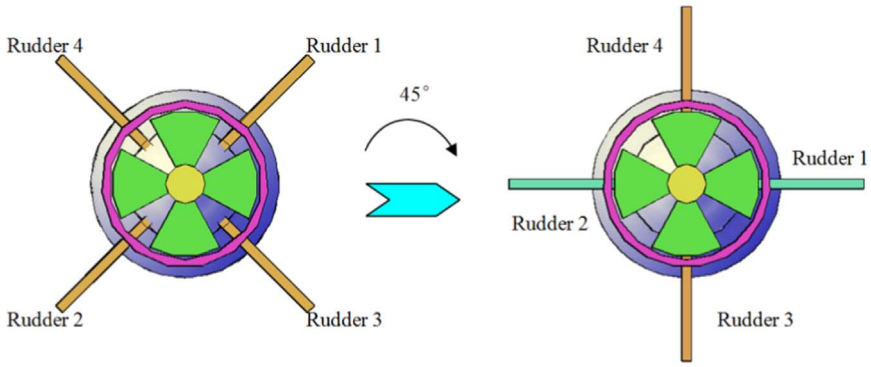

Fig. 9. The transportation from X rudder to cross rudder.

Table 4
Main parameters of the cross rudder and calculation process.

	Value	Calculation process	Effects on control performance
$X_{\delta_H\delta_H}$	-1.0061×10^{-3}	$X_{\delta_H\delta_H} = X_{\delta_1\delta_1} + X_{\delta_2\delta_2}$	The effect of horizontal rudder's operation to X in $\boldsymbol{\tau}$
$X_{\delta_V\delta_V}$	-1.1290×10^{-3}	$X_{\delta_V\delta_V} = X_{\delta_3\delta_3} + X_{\delta_4\delta_4}$	The effect of vertical rudder's operation to X in $\boldsymbol{\tau}$
Y_{δ_V}	-1.6938×10^{-3}	$Y_{\delta_V} = 2\times(\lvert Y_{\delta_4}\rvert \times COS(\pi/4) + \lvert Z_{\delta_4}\rvert \times COS(\pi/4))\times(-1)$	The effect of vertical rudder's operation to Y in $\boldsymbol{\tau}$
Z_{δ_H}	-1.4821×10^{-3}	$Z_{\delta_H} = 2\times(\lvert Z_{\delta_1}\rvert \times COS(\pi/4) + \lvert Y_{\delta_1}\rvert \times COS(\pi/4))\times(-1)$	The effect of horizontal rudder's operation to Z in $\boldsymbol{\tau}$
M_{δ_H}	-1.5360×10^{-4}	$M_{\delta_H} = 2\times(\lvert M_{\delta_1}\rvert \times COS(\pi/4) + \lvert N_{\delta_1}\rvert \times COS(\pi/4))\times(-1)$	The effect of horizontal rudder's operation to M in $\boldsymbol{\tau}$
N_{δ_V}	1.9269×10^{-4}	$N_{\delta_V} = 2\times(\lvert M_{\delta_4}\rvert \times COS(\pi/4) + \lvert N_{\delta_4}\rvert \times COS(\pi/4))$	The effect of vertical rudder's operation to N in $\boldsymbol{\tau}$

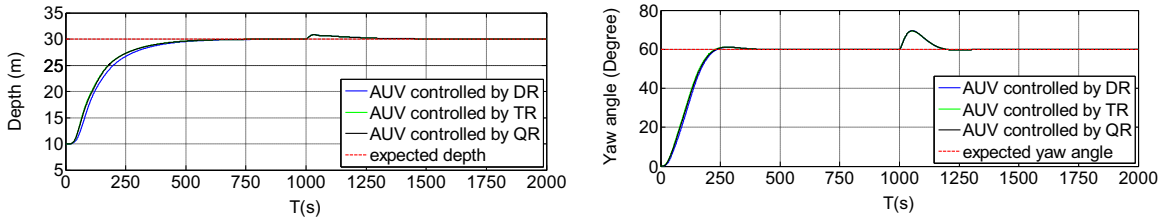

(a) Depth control (b) Yaw control

Fig. 10. X-rudder AUV's control results under instantaneous disturbance (a) Depth control (b) Yaw control.

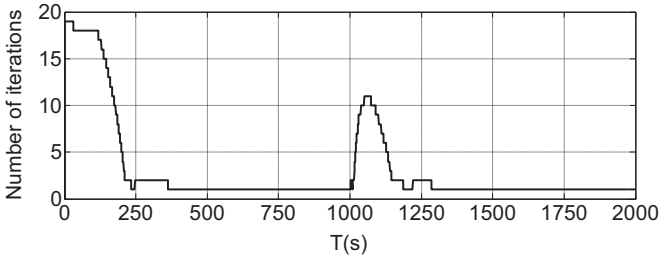

Fig. 11. Number of iterations during QR control under instantaneous disturbance.

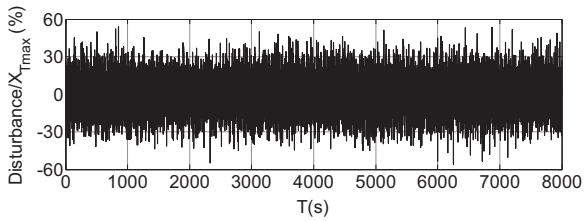

Fig. 12. Relative value of random disturbance.

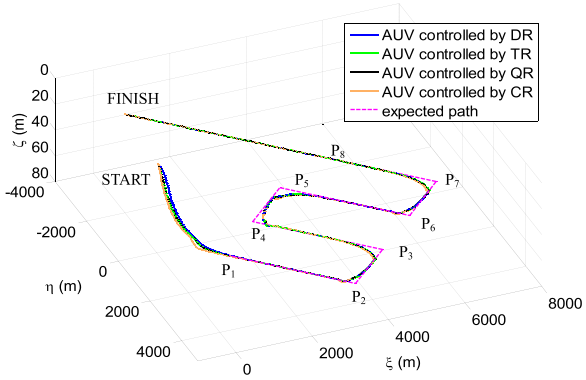

Fig. 13. X-rudder AVU's path following results under random disturbance.

one cross rudder control, which is transformed from X rudder, in order to make a comprehensive test for X rudder's control ability. The whole path following process can be separated into two main parts: one is the control from AUV's start point to expected depth (60m) by certain yaw angle (30°), the other one is AUV following the certain path after reaching the desired depth. The path following control is based on the line of sight guidance method (Ataei, 2014).

Before the control ability comparison of X rudder and cross rudder, we need to find a proper way of transforming an X-rudder AUV to a cross-rudder AUV. We decide to make the changes shown as Fig. 9. After the changes, the horizontal rudder in cross rudder is related to Rudder 1 and Rudder 2 in X rudder. And the vertical rudder in cross rudder is related to Rudder 3 and Rudder 4 in X rudder.

According to dynamics and Table 2 in Section 2.3, we can approximately calculate the corresponding main parameters of this new cross-rudder AUV. The main parameters of this cross rudder and

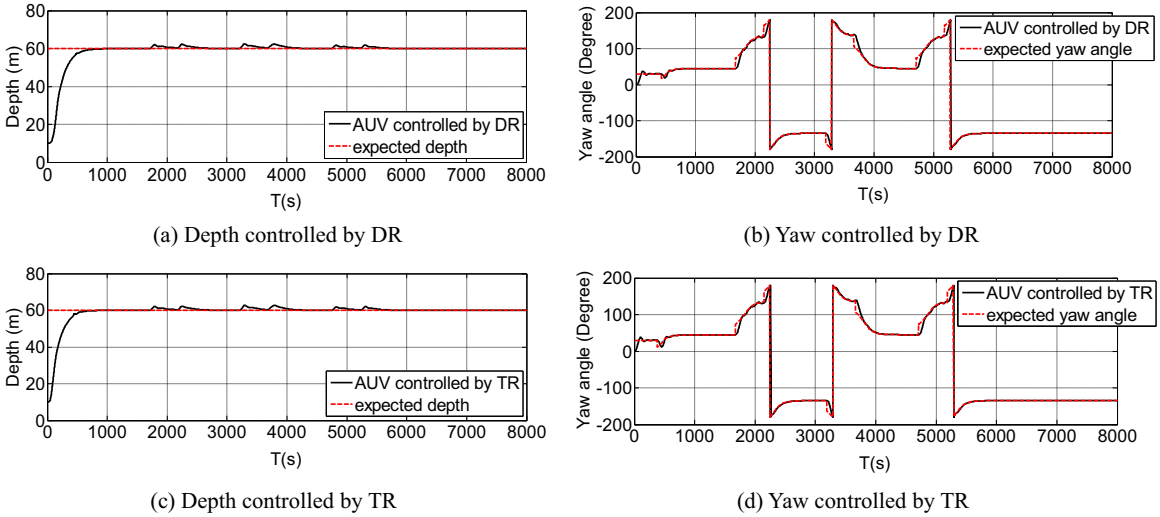

(a) Depth controlled by DR (b) Yaw controlled by DR

(c) Depth controlled by TR (d) Yaw controlled by TR

Fig. 14. Depth and yaw control results by rudder allocation of X rudder and cross rudder under random disturbance (a) Depth controlled by DR (b) Yaw controlled by DR (c) Depth controlled by TR (d) Yaw controlled by TR (e) Depth controlled by QR (f) Yaw controlled by QR (g) Depth controlled by CR (h) Yaw controlled by CR.

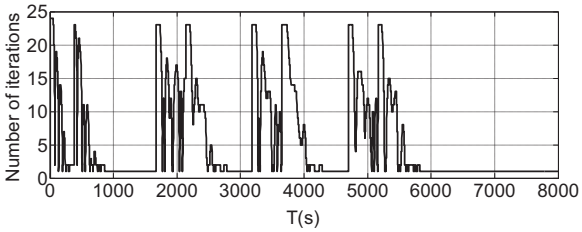

Fig. 15. Number of iterations during QR control under random disturbance.

the calculation process are shown in Table 4.

This new cross rudder's influence to AUV's $\boldsymbol{\tau}$ in Eq. (2) is shown in Eq. (19) and its control information framework is shown in Fig. 3 in Section 3.1.

$$\begin{cases} X = X_{\delta_H\delta_H} \times u^2 \times {\delta_H}^2 + X_{\delta_V\delta_V} \times u^2 \times {\delta_V}^2 \\ Y = Y_{\delta_R} \times u^2 \times \delta_R \\ Z = Z_{\delta_H} \times u^2 \times \delta_H \\ M = M_{\delta_S} \times u^2 \times \delta_S \\ N = N_{\delta_V} \times u^2 \times \delta_V \end{cases} \tag{19}$$

As to the control law for controllers, we will use PID control method and S control method to show X rudder allocation's performance in two simulations. PID (Fuyang, 2010) control method is widely used in engineering field. It can be described as Eq. (20).

$$u_{out} = K_P \times e + K_I \times \int e dt + K_D \times \dot{e},\ K_P, K_I, K_D \in R \tag{20}$$

Where

K_P, K_I and K_D are adjustable parameters. e is the error between control result and expected value. $\dot{e}$ is the change rate of e. PID controller is one linear controller.

S control method (XM and YR, 2001) is based on the structure of PID control method and combines the thought of fuzzy logic. S control method can be described as Eq. (21).

$$u_{out} = 2/(1 + e^{(-1\times k_1\times e - 1\times k_2\times \dot{e})}) + k_3,\ k_1, k_2 \in R_+,\ k_3 \in R \tag{21}$$

Where

e is the error between control result and expected value. $\dot{e}$ is the change rate of e. k_1,k_2 and k_3 are adjustable parameters. If the control result has overshoot, we can decrease k_1 and increase k_2. If the control result's convergence time is very long, we can increase k_1 and decrease k_2. If the control result has steady-state error, it can be adjusted by the change of k_3 (Tang Xudong, 2009). S control method has been used on AUV in tank experiment and sea experiment for many times. Its stability analysis is given by Li (2013), so we won't explain it here. S controller is one nonlinear controller.

4.2. Simulation and results

In simulations, we make the following assumptions and arrangements:

- AUV is neutrally buoyant.
- Considering the complex relationship between environmental disturbance and flow velocity, we assume flow velocity to rudder is approximately equal to AUV's velocity in Eq. (17).
- As to the rudder allocation of X rudder, DR's performance in simulation is generated by Rudder 1 and Rudder 3. TR's performance in simulation is generated by Rudder 1, Rudder 2 and Rudder 3. QR's performance in simulation is generated by Rudder 1, Rudder 2, Rudder 3 and Rudder 4.
- The common adjustable parameters in different X rudder allocation are the same, for instance the parameters in corresponding PID controllers and S controllers in DR, TR and QR are the same. As to the parameters in corresponding S controllers of the cross-rudder AUV, they are set independently in order to getting the proper control ability.
- In two simulations, AUV's original state is static. Its original yaw angle , pitch angle and all of rudder's angle are 0°. The maximum angular velocity of every rudder in X rudder and cross rudder is 1°/s. The angle range of every rudder in X rudder and cross rudder is from −35° to +35°. AUV's expected u is $6kn$ and its start point is (0,0,10) in $\{N\}$.

4.2.1. X-rudder AUV's simulation by PID controller under instantaneous disturbance

In this part, we test X rudder's allocation by finishing one certain movement in the environment with instantaneous disturbance. We set disturbance as the twice value of the maximum value of the main thruster and its direction is $\overrightarrow{E\xi}$. The instantaneous disturbance will last for 2 s. PID controller is used in this simulation.

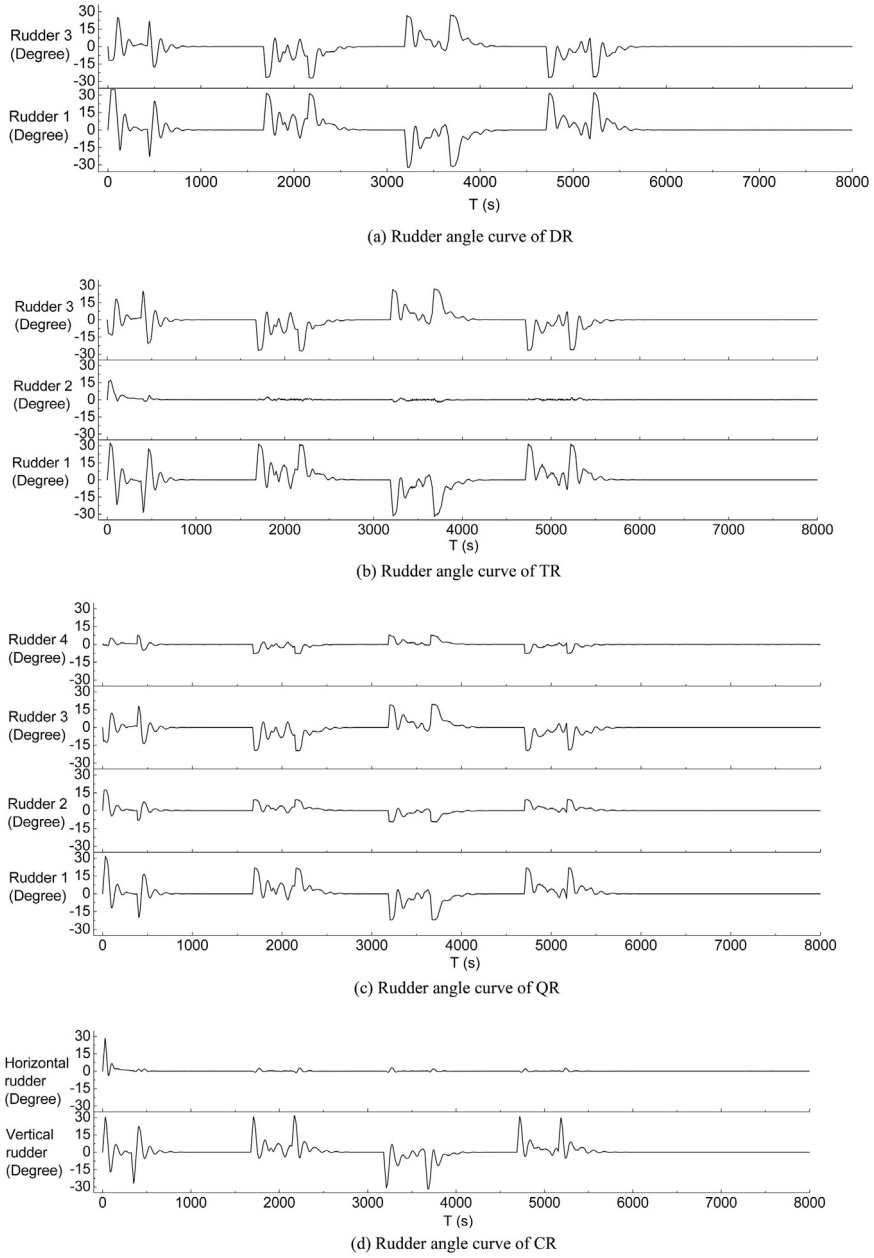

Fig. 16. Rudder angle curve by rudder allocation of X rudder and cross rudder control (a) Rudder angle curve of DR (b) Rudder angle curve of TR (c) Rudder angle curve of QR (d) Rudder angle curve of CR.

The certain movement is to change the depth and yaw angle at the same time. The expect depth is 30 m and the expected yaw angle is 60°. Runtime of this simulation is 2000 s and the instantaneous disturbance happens at $1000s$. The value of the instantaneous disturbance is nearly two times larger than the main thruster's maximum value. The main parameters in QR are set as follows, $\boldsymbol{W}_v = diag(1/35,\ 1/35,\ 1/35)$, $\boldsymbol{W}_u = diag(1/35,\ 1/35,\ 1/35,\ 1/35)$, $\varepsilon = 0.5$ and $J_{end} = 0.00125$. The simulation results are shown in Fig. 10.

Fig. 10 shows all the X rudder's allocation can cooperate well with PID controller. DR, TR and QR can make AUV achieve the expected depth and yaw. As to depth control, the overshoot of DR, TR and QR is 0.86 m, 0.83 m and 0.81 m. As to yaw control, the overshoot of DR, TR and QR is 9.55°, 9.37° and 9.40°. These three X rudder's allocation modes have nearly the same control accuracy in this situation. With the help of X rudder allocation and PID controller, X rudder can finish the task under the instantaneous disturbance. Fig. 11 shows QR's iteration number. We can notice that the center computer's work load is not very high.

4.2.2. X-rudder AUV's simulation by S controller under random disturbance

In this part, we test X rudder's allocation by a path following mission in the environment with random disturbance. We set the disturbance in direction of $\overrightarrow{E\xi}$ and $\overrightarrow{E\eta}$. Fig. 12 shows the random disturbance and its value is shown by the percentage of disturbance/ $X_{T\ \max}$. $X_{T\ \max}$ is the maximum value of the main thruster. S controller is used in this simulation.

The expected lawn mower path is the connection of P_1 (1050,1850,60), P_2 (3450,4250,60), P_3 (4650,3050,60), P_4 (2250,650,60), P_5 (3450,−550,60), P_6 (5850,1850,60), P_7 (7050,650,60) and P_8 (4650,−1750,60) in $\{N\}$. The sample interval is $0.5s$. Runtime of this situation is 8000 s. The main parameters in QR are the same as those in 4.2.1.

In order to simplify representation in this part, CR is short for cross rudder. The simulation results are shown in Figs. 13 and 14.

Figs. 13 and 14 show that all of the X rudder control methods and

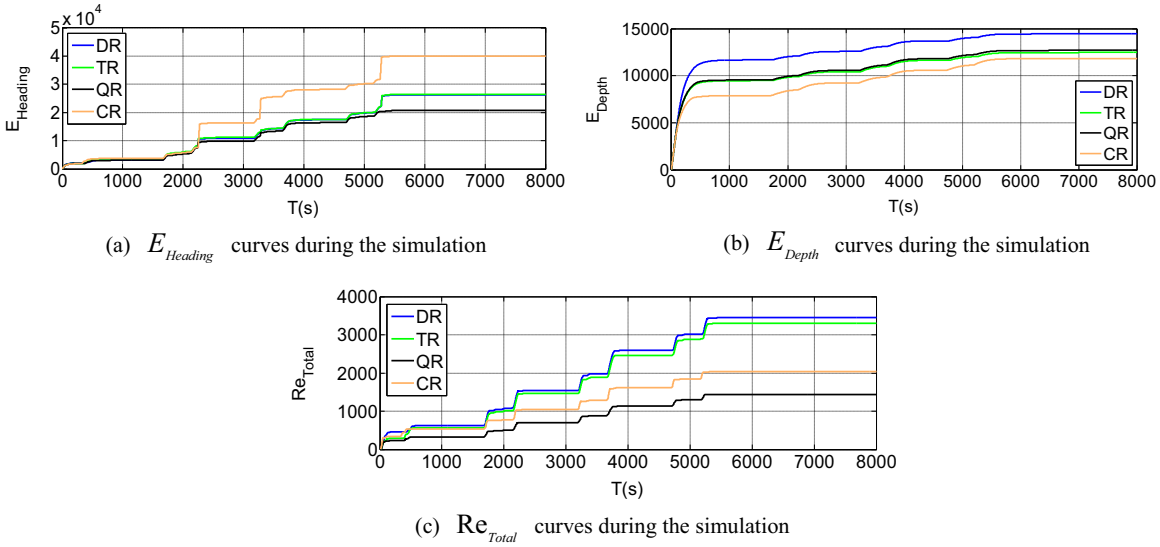

(a) $E_{Heading}$ curves during the simulation

(b) E_{Depth} curves during the simulation

(c) Re_{Total} curves during the simulation

Fig. 17. Results of X rudder's and cross rudder's control ability judgment (a) $E_{Heading}$ curves during the simulation (b) E_{Depth} curves during the simulation (c) Re_{Total} curves during the simulation.

Table 5
Summary of corresponding values for judgment.

	M_w	DR	TR	QR	CR
$E_{Heading}$	0.25	26,278	26,462	20,750	40,063
E_{Depth}	0.25	14,481	12,488	12,726	11,826
Re_{Total}	0.5	3444	3300	1442	2031

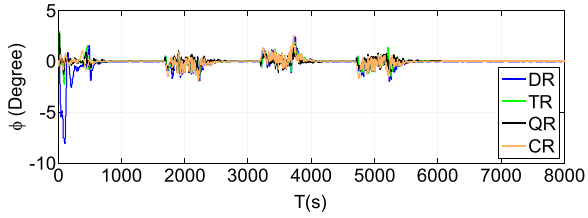

Fig. 18. AUV'S roll angle influenced by rudder allocation of X rudder.

the cross rudder control can complete the mission efficiently and stably. X-rudder AUV can achieve the mission used to be completed by cross-rudder AUV. DR, TR and QR can achieve the depth and heading control, which also means that the anti-normalization is useful. Fig. 15 shows that the number of iterations doesn't increase forever, which means the fixed point iteration we designed in Section 3.3.3 can run well and Eq. (14) satisfies the condition of the contraction mapping theorem.

Fig. 16 shows the rudder curves of different X rudder allocation modes and the cross rudder during the whole mission. It shows how the AUV works under random disturbance. When AUV gets to the path following part, the maximum absolute values of rudders in DR, TR, QR and CR are 32.3° at 3228.5 s, 32.0° at 3687.5 s, 22.2° at 5196 s and 31.9° at 3686.5 s. As to these singles of rudder's operation, QR's operation is the least.

If we want to compare DR, TR, QR and CR in a more intuitive way, we can use the control ability judgment offered in Section 3.4 to find out which control method is the best. As the rudders are all operated in the same environment, we can set $\rho = 1$ in both X rudder's judgment and cross rudder's judgment. Considering that every rudder's appearances in X rudder are the same and the test cross rudder is transformed from X rudder, we can set every rudder's $S_{rudder} = 1$ in X rudder's judgment and every rudder's $S_{rudder} = 2$ in cross rudder's judgment. Considering that the final judgment results are normalized and to make it simpler, we don't mention the measurement units of every value here, which will not influence the final results. Corresponding value's curves about judgment are shown in Fig. 17 and the summary is shown in Table 5. In Eq. (17), we set $\boldsymbol{M}_w = [0.250.250.5]$. It means that we treat traditional judgment standard and resistance energy equal in the final judgment.

As to double-rudder allocation, the final judgment result is

$$A_{DR} = [0.25 \quad 0.25 \quad 0.5] \bullet [26278/40063 \quad 14481/14481 \quad 3444/3444]^T = 0.914.$$

As to triple-rudder allocation, the final judgment result is

$$A_{TR} = [0.25 \quad 0.25 \quad 0.5] \bullet [26462/40063 \quad 12488/14481 \quad 3300/3444]^T = 0.860.$$

As to quadruple-rudder allocation, the final judgment result is

$$A_{QR} = [0.25 \quad 0.25 \quad 0.5] \bullet [20750/40063 \quad 12726/14481 \quad 1442/3444]^T = 0.559.$$

As to cross rudder control, the final judgment result is

$$A_{CR} = [0.25 \quad 0.25 \quad 0.5] \bullet [40063/40063 \quad 11826/14481 \quad 2031/3444]^T = 0.749.$$

So, $A_{QR} < A_{CR} < A_{TR} < A_{DR}$. A_{QR} has the least value in A_{DR},A_{TR},A_{QR} and A_{CR}. According to the judgment we designed, quadruple-rudder allocation has the best control ability in this mission. Besides that, QR also has the least Re_{Total}, which means the AUV operated by this X rudder control method can have the least rudder operation and maybe can run the longest time in all of the methods mentioned here.

As to the roll angle, the control results are shown in Fig. 18. The separate maximum absolute values of roll angles controlled by DR, TR, QR, and CR are respectively 7.99°, 2.96°, 2.63° and 2.79° during the whole mission. When the AUV gets to the part of path following, the maximum absolute value of roll angles controlled by X rudder is less than 2.38° and QR's maximum absolute value of roll angles is the least according to Fig. 18. The less roll angle of AUV means the better stability of AUV's movement. It can provide the sensors, such as multi-beam sonar, camera and DVL, with a better working condition.

So, according to the judgment in Section 3.4 and the control results of AUV's roll angle, QR is the best choice in this lawn mower path following mission. Besides PID controller, we can notice that X rudder's allocation methods we designed in this paper can also work well with S controller, under random disturbance. The simulation results show that the designed X rudder control method has the robustness.

5. Conclusions

For the X rudder's use in AUV's motion control, three main opinions are proposed to solve that problem in this paper. They are the anti-normalization method based on virtual rudder, rudder allocation and the judgment method about control ability with the consideration of rudder's operation and control accuracy. As to the rudder allocation, it contains three modes, which are double-rudder mode, triple-rudder mode and quadruple-rudder mode. Their characters can be summed up as follows:

- Double-rudder mode is under-actuated. The control method is understandable and easy.
- Triple-rudder mode is full-actuated. The control method is comprehensible.
- Quadruple-rudder mode is over-actuated. The control method tries to use the least rudder's operation to finish missions. Although quadruple-rudder mode is more complex than double-rudder mode and triple-rudder mode in design, it is not difficult in the use of mission's operation.

The simulations show that the anti-normalization method and rudder allocation can work well. No matter the rudder allocation cooperates with PID controller or S controller, it can make X-rudder AUV complete the mission under the environment with instantaneous or random disturbance. In the lawn mower path following mission, the comparison between X rudder and cross rudder AUVs presents X rudder's quadruple-rudder allocation can help AUV finish the task with high accuracy and low energy consumption caused by rudder's operation. Even though our simulations are based on X-rudder AVU's working environment, we can't deny the differences between simulation and reality. In the future, if enough funds, we would do field tests and pay more attention to these three points. The first point is to optimize the X rudder allocation, especially the parameter's setup in quadruple-rudder mode, which can be convenient for the users with little experience in AUV's control. The second point is to research the cooperation of X rudder allocation and other complex controllers, such as a robust sliding-mode feedback controller (ChengS, 2013) and a self-constructing adaptive robust fuzzy neural controller (Ning, 2015). The third point is to study the fault-tolerant control of X-rudder AUV, such as the effect of rudder-jamming. X rudder's redundancy has great advantages in this field, which by no means can be achieved by cross rudder. We believe that these studies can reveal the great potential of X-rudder AUVs.

Acknowledgement

This research is supported by Ministry of Science and Technology of the People´s Republic of China, No. 51509057 and National 863 High Technology Development Plan Project of China, No. 2011AA09A106. It has also been partially supported by China Postdoctoral Science Foundation, No. 2012T50331. Great thanks are addressed to them by the research team.

References

Ataei, M., 2014. Three-dimensional optimal path planning for waypoint guidance of an autonomous underwater vehicle. Robot. Auton. Syst. 67, 23–32.
Burken, J.J., et al., 2001. Two reconfigurable flight-control design methods: robust servomechanism and control allocation. J. Guid. Control Dyn. 24, 482–493.
Cheng, Michael, 2012. Modeling and testing of hydrodynamic damping model for a complex-shaped remotely-operated vehicle for control. J. Mar. Sci. Appl. 11 (2), 150–163.
ChengS, Chin, et al., 2013. Sliding-mode control of an electromagnetic actuated conveyance system using contactless sensing. IEEE Trans. Ind. Electron. 60 (11), 5315–5324.
Chin, C.S., et al., 2008. Robust and decoupled cascaded control system of underwater robotic vehicle for stabilization and pipeline tracking. Proc. Inst. Mech. Eng. Part I: J. Syst. Control Eng. 222 (4), 261–278.
Chin, C.S., et al., 2011. Rapid modeling and control systems prototyping of a marine robotic vehicle with model uncertainties using xPC Target system. Ocean Eng. 38 (17), 2128–2141.
Chun, R.D., 2012. Fixed Point Theory and Applications. National Defense Industry Press, China.
Fang, Wang, et al., 2010. A survey on development of motion control for underactuated AUV. Shipbuild. China 51 (2), 228–241.
Fossen, T., 2002. Marine Control Systems. Marine Cybernetics, Norwaay.
Fossen, T., 2011. Handbook of Marine Craft Hydrodynamics and Motion Control. Jhon Wiley & Sons Ltd., United Kingdom.
Fuyang, Chen, et al., 2010. Principles of Automatic Control. National Defence Industry Press, China.
Gotland-Class Submarine. ⟨https://en.wikipedia.org/wiki/Gotland-class_submarine⟩.
Hagen, P.E., et al., 2006. The HUGIN AUV for Force Protection in the Littorals.
Jon, Crowell, 2013. Design challenges of a next generation small AUV. In: OCEANS 2013 MTS/IEEE.
Lapierre, L., Jouvencel, B., 2008. Robust nonlinear path-following control of an AUV. IEEE J. Ocean. Eng. 33 (2), 89–102.
Lee, Billingham, 2004. The role of inspection and intervention AUVs in support of the oil fields of the future. J. Offshore Technol. 12 (6), 47.
Lei, W.A.N., et al., 2015. AUV's bottom following control method based on ADRC. Axta Armament. 36 (10), 1943–1948.
Li, Y.M., , et al.2013. Stability analysis on S plane control of underwater vehicles. In: Proceedings of the 2nd International Conference on Industrial Design and Mechanics Power, pp. 716–721.
Ma, H.W., et al., 2015. A biomimetic cownose ray robot fish with oscillation and chordwise twisting flexible pectoral fins. Ind. Robot Int. J. 42, 214–221.
Negre, Carrasco Pep Lluis, et al., 2014. Stereo graph-SLAM for autonomous underwater vehicles. Adv. Intell. Syst. Comput. 302, 351–360.
Nina, Mahmoudian, et al., 2010. Approximate analytical turning conditions for underwater gliders: implications for motion control and path planning. IEEE J. Ocean. Eng. 35 (1), 131–143.
Ning, Wang, et al., 2015. Self-constructing adaptive robust fuzzy neural tracking control of surface vehicles with uncertainties and unknown disturbances. IEEE Trans. Control Syst. Technol. 23 (3), 991–1002.
Park, B.S., 2015. Adaptive formation control of underactuated autonomous underwater vehicles. Ocean Eng. 96, 1–7.
Ri, Ge, Tu, Le, et al., 2015. The design and production of thrusters for an AUV without rudders. In: Proceedings of the Control Conference (ASCC).
Sang-Ki, Jeong, et al., 2016. Design and control of high speed unmanned underwater glider. Int. J. Precis. Eng. Manuf.-Green. Technol. 3 (3), 273–279.
Shengda, Shi, 1995. Submarine Maneuverability. National Defence Industry Press, China.
Sōryū-Class Submarine. ⟨https://en.wikipedia.org/wiki/S%C5%8Dry%C5%AB-class_submarine⟩.
Tadahiro, Hyakudome, et al., 2012. Development of AUV for scientific observation. In: OCEANS 2012 MTS/IEEE.
Tang Xudong, et al., 2009. Improved PSO and its application research on tuning of S plane parameters in AUV's motion control. J. Basic Sci. Eng. 17 (1), 153–160.
Tao, L.I.U., et al., 2002. "CR-02" 6000 m AUV hull structure systems. J. Ship Mech. 6 (6), 114–119.
Tiansen, Li, 2007. Torpedo Manoeuvrability Second edition. National Defence Industry Press, China.
Type 212 Submarine. ⟨https://en.wikipedia.org/wiki/Type_212_submarine⟩.
Volker, B., 2000. Practical Ship Hydrodynamics. Butterworth-Heinemann, United Kingdom.
Wei-feng, Ma, et al., 2008. Current researches and development trend on AUV. Fire Control Command Control 33 (6), 10–13.
XM, L.I.U., YR, X.U., 2001. S control of automatic underwater vehicles. Ocean Eng. 19 (3), 81–84.
Yoshida, Hiroshi , et al., 2013. An autonomous underwater vehicle with a canard rudder for underwater minerals exploration. In: Proceedings of the 2013 IEEE International Conference on Mechatronics and Automation. pp. 1571–1576.